Positive regulation of plasmacytoid dendritic cell function via Ly49Q recognition of class I MHC

Lee-Hwa Tai,[1,2] Marie-Line Goulet,[1,2] Simon Belanger,[1,2] Noriko Toyama-Sorimachi,[3] Nassima Fodil-Cornu,[4] Silvia M. Vidal,[2,4] Angela D. Troke,[1,2] Daniel W. McVicar,[5] and Andrew P. Makrigiannis[1,2]

[1]Laboratory of Molecular Immunology, Clinical Research Institute of Montréal, Montréal, Quebec H2W 1R7, Canada
[2]Department of Microbiology and Immunology, McGill University, Montréal, Quebec H3G IY6, Canada
[3]Department of Gastroenterology, Research Institute, International Medical Center of Japan, Shinjuku-ku, Tokyo 162-8655, Japan
[4]Department of Human Genetics and McGill Centre for the Study of Host Resistance, McGill University, Montréal, Quebec H3A 2B4, Canada
[5]Cancer and Inflammation Program, Laboratory of Experimental Immunology, Center for Cancer Research, National Cancer Institute at Frederick, Frederick, MD 21702

Plasmacytoid dendritic cells (pDCs) are an important source of type I interferon (IFN) during initial immune responses to viral infections. In mice, pDCs are uniquely characterized by high-level expression of Ly49Q, a C-type lectin-like receptor specific for class I major histocompatibility complex (MHC) molecules. Despite having a cytoplasmic immunoreceptor tyrosine-based inhibitory motif, Ly49Q was found to enhance pDC function in vitro, as pDC cytokine production in response to the Toll-like receptor (TLR) 9 agonist CpG-oligonucleotide (ODN) could be blocked using soluble monoclonal antibody (mAb) to Ly49Q or H-2K^b. Conversely, CpG-ODN–dependent IFN-α production by pDCs was greatly augmented upon receptor cross-linking using immobilized anti-Ly49Q mAb or recombinant H-2K^b ligand. Accordingly, Ly49Q-deficient pDCs displayed a severely reduced capacity to produce cytokines in response to TLR7 and TLR9 stimulation both in vitro and in vivo. Finally, TLR9-dependent antiviral responses were compromised in Ly49Q-null mice infected with mouse cytomegalovirus. Thus, class I MHC recognition by Ly49Q on pDCs is necessary for optimal activation of innate immune responses in vivo.

CORRESPONDENCE
Andrew P. Makrigiannis:
makriga@ircm.qc.ca

Abbreviations used: B6, C57BL/6; BAC, bacterial artificial chromosome; BST2, bone marrow stromal cell antigen 2; DOTAP, 1,2-dioleoyloxy-3-trimethylammonium-propane; ES, embryonic stem; ITAM, immunoreceptor tyrosine-based activation motif; ITIM, immunoreceptor tyrosine-based inhibitory motif; mDC, myeloid DC; MCMV, mouse CMV; MFI, mean fluorescence intensity; mPDCA-1, mouse PDC antigen 1; ODN, oligonucleotide; pDC, plasmacytoid DC; SHP, Src homology phosphatase; TLR, Toll-like receptor.

Plasmacytoid DCs (pDCs) are potent antiviral effector cells that were originally identified by their plasma cell–like morphology and localization within the T cell zone of lymphoid tissue (1). Also termed type I IFN-producing cells, pDCs secrete more type I IFN on a per-cell basis than any other cell type (2–4). pDCs are especially important in controlling viral infections, a property highlighted by their selective expression of Toll-like receptor (TLR) 7 and TLR9 (5), which recognize single-stranded RNA and double-stranded DNA, respectively. pDCs do not express TLR2, TLR3, TLR4, and TLR5, explaining why they do not respond to common bacterial products recognized by other APCs.

pDCs represent a rare cell type constituting ∼1% of bone marrow or splenic leukocytes and <0.5% of lymph node and peripheral blood leukocytes. However, their frequency varies between mouse strains with 129Sv mice possessing a significantly higher proportion of pDCs than other mouse strains (6). Mouse pDCs do not express the lineage markers CD19, CD3, DX5, CD14, or TER119 (7, 8). In addition to their selective pattern of TLR expression, pDCs and myeloid DCs (mDCs) are dissimilar in various other aspects. Unlike mDCs, pDCs are characterized by a CD11b$^-$B220$^+$Ly6C$^+$ phenotype (7). Like mDCs, pDCs express CD11c but they do so at a lower level (8). Resting pDCs have been referred to as immature APCs because they express only low levels of CD86 and class II MHC, and they display little or no endocytic

L.-H. Tai and M.-L. Goulet contributed equally to this paper.

The Rockefeller University Press $30.00
J. Exp. Med. Vol. 205 No. 13 3187-3199
www.jem.org/cgi/doi/10.1084/jem.20080718

activity. However, upon TLR stimulation all three of these characteristics are up-regulated to allow pDCs to present antigenic peptides and optimally stimulate $CD4^+$ T cell function (7). In addition, pDCs have been implicated in promoting mDC maturation and terminal B cell differentiation to functional antibody-producing plasma cells (1). Five different mAb reagents have been reported to specifically recognize mouse pDCs: 120G8 (6), mouse PDC antigen 1 (mPDCA-1), 440c (9), NS-34 (10), and 2E6 (11). The 440c mAb recognizes Siglec-H, a DAP12-coupled receptor that inhibits pDC function, including IFN-α secretion (12). 120G8 and mPDCA-1 both recognize bone marrow stromal cell antigen 2 (BST2) (13). NS-34 and 2E6 recognize Ly49Q, a member of the type II C-type lectin-like Ly49 family. Interestingly, most other Ly49 family members are exclusively expressed on NK, NKT, and T cell subsets, where they are known to regulate cytokine production and cell-mediated cytotoxicity via interactions with cognate class I MHC–related ligands on target cells.

Ly49Q is one of the more distantly related Ly49 family members, yet the receptor itself is highly conserved among three mouse haplotypes (C57BL/6 [B6], 129S6, and BALB/c) (14–16). To date, Ly49Q protein has been detected in all mouse strains tested (17), suggesting an important and conserved function for this receptor. The *Ly49q* gene defines the centromeric end of the B6, 129S6, and BALB/c *Ly49* gene clusters. Interestingly, a homologous segment comprising *Ly49q*- and *Ly49e*-like genes is repeated three times in the 129S6 genome because of gene duplication (18). Therefore, in addition to $Ly49q_1$, the 129-related mouse strains contain $Ly49q_2$ and $Ly49q_3$, but the latter two genes are considered pseudogenes because they lack exons 6 and 7, which encode the ligand-binding domain (18).

Ly49Q was first reported to be expressed at low levels on a proportion of $Gr\text{-}1^+$ bone marrow myeloid precursor cells, on peripheral blood neutrophils ($Gr1^+CD11b^+$), and on IFN-γ–activated macrophages (10). However, the function of the receptor on these cell types remains unknown. Ly49Q contains a cytoplasmic immunoreceptor tyrosine-based inhibition motif (ITIM), whereas it lacks a positively charged transmembrane residue, both of which are characteristics of inhibitory Ly49 receptors expressed by NK cells. Furthermore, similar to inhibitory Ly49 NK receptors, the Ly49Q ITIM has been reported to associate with the Src homology phosphatases (SHPs) 1/2 upon antibody-mediated cross-linking of the receptor (10). However, Ly49Q is not expressed by NK cells. Moreover, Ly49Q cross-linking on activated macrophages has been reported to induce cytoskeletal rearrangement leading to formation of polarized filopodia and lamellopodia; this suggests a role for Ly49Q in macrophage migration and phagocytosis (10).

In subsequent reports, a population of cells expressing significantly higher levels of Ly49Q than neutrophils and macrophages was identified (11, 17, 19). This cell population was originally defined as $CD11c^+B220^+Gr1^{low}$ and has been confirmed to represent pDCs (1, 20). Virtually all peripheral pDCs and the majority of bone marrow pDCs express Ly49Q. The subset of bone marrow pDCs lacking Ly49Q expression are thought to represent immature cells, such that acquisition of Ly49Q expression is linked to sequential development of functional pDCs (11, 19). These $Ly49Q^-$ pDCs do not respond to certain stimuli and are defective in the secretion of some cytokines. Ly49Q levels correlate well with pDC maturation, and receptor acquisition is further up-regulated by various stimuli, including IFN-α (17, 19). In some but not all inbred mouse strains, a subset of mDCs also expresses low levels of Ly49Q (17).

We recently identified the classical class I MHC molecule, $H\text{-}2K^b$, as the cognate Ly49Q ligand (21). Using reporter cell analysis, a high-affinity ligand for Ly49Q was detected on tumor and normal ex vivo cells derived from $H\text{-}2^b$ haplotype mice (B6 and 129) but not on cells from the other mouse MHC haplotypes tested. Direct MHC surveillance by pDCs and the implications of this interaction for innate immunity remain to be investigated.

The current study demonstrates a major role for Ly49Q–$H\text{-}2K^b$ interactions in pDC production of IFN-α and, to a lesser extent, IL-12. Remarkably, the function of Ly49Q on pDCs appears to be stimulatory in nature, as revealed by cross-linking experiments despite the presence of a cytoplasmic ITIM. To confirm these in vitro findings and to ascertain the role of Ly49Q during immune responses, Ly49Q-null mice were generated and characterized. Ly49Q-null mice exhibit a severe defect in systemic IFN-α production after challenge with agonists and pathogens recognized by TLR7 and TLR9, which translates into weaker antiviral responses in vivo. We propose that Ly49Q recognition of self-MHC is necessary to regulate pDC cytokine responses to pathogens.

RESULTS

Ly49Q interactions with class I MHC are necessary for IFN-α secretion by pDCs

We have previously shown that $H\text{-}2K^b$ is a ligand for Ly49Q (21), suggesting that pDC function may be regulated by class I MHC. Therefore, we investigated the influence of Ly49Q–class I MHC interactions on type I IFN secretion by pDCs in response to innate immune stimuli. As previously reported, overnight culture of splenic pDCs (129S1 strain) in the presence of CpG-oligonucleotide (ODN resulted in robust IFN-α production (6). However, when blocking mAb (21) specific for either Ly49Q or $H\text{-}2K^b$ were added at the initiation of cell cultures, IFN-α secretion by pDCs was almost completely abrogated (Fig. 1 A). IL-12 secretion by pDCs could also be blocked using Ly49Q or $H\text{-}2K^b$ mAb (Fig. 1 B). Thus, interaction of the ITIM-containing Ly49Q receptor with cognate $H\text{-}2K^b$ ligand appears to be necessary for efficient TLR9-induced cytokine production by pDCs.

To test the possibility that Ly49Q is directly involved in activating pDCs and stimulating IFN-α production upon receptor ligation, plate-bound mAb-mediated cross-linking experiments were used. Because pDCs from B6 mice are low producers of type I IFN compared with 129 mice (6), B6 pDCs were selected to enhance detection of increased IFN secretion. As previously reported, B6 pDCs cultured in the presence of

CpG-ODN produced low levels of IFN-α. In contrast, when B6 pDCs were cultured on immobilized Ly49Q mAb, IFN-α production was increased 10–15-fold (Fig. 1 C). IFN-α secretion was also induced using immobilized recombinant ligand (K^b:Ig/OVA) showing that MHC directly activates pDCs. When this experiment was repeated with 129S1-derived pDCs, anti-Ly49Q cross-linking also significantly increased IFN-α production in response to CpG-ODN, albeit to a lesser extent (Fig. 1 E). Collectively, these results suggest that pDCs are synergistically activated by class I MHC and TLR9 ligands.

The activation of pDCs through Ly49Q, an ITIM-bearing receptor, contrasts with the established functions of similar receptors in lymphocytes. However, our findings are complementary to those of recent studies reporting that immunoreceptor tyrosine-based activation motif (ITAM)-coupled receptors inhibit pDC activation, specifically IFN-α production (12, 22). To determine the outcome of simultaneous ITIM- and ITAM-mediated signal transduction in pDCs, purified cells were cultured in the presence of CpG-ODN on immobilized anti-Ly49Q, anti–Siglec-H (a DAP12-coupled receptor), or both. Using both B6- and 129-derived pDCs, inhibitory Siglec-H cross-linking blocked Ly49Q activation and suppressed IFN-α secretion (Fig. 1, D and E). Notably, the reported inhibitory effect of anti–Siglec-H was only seen with 129-derived pDCs, likely because of the larger basal IFN-α response seen using 129 versus B6 strain pDCs. Thus, ITAM-mediated inhibitory signals appear to be dominant and suppress ITIM-mediated stimulatory signals in pDCs.

Targeted disruption of the *Ly49q$_1$* gene

To confirm the role of Ly49Q in pDC function, we sought to determine the effect of Ly49Q deficiency by targeted gene disruption in vivo. The *Ly49q$_1$* gene was disrupted in 129-background embryonic stem (ES) cells by inserting a floxed neomycin cassette into the StuI site of exon 2 adjacent to the ITIM coding region (Fig. 2 A). Founder mice shown to carry the *Ly49q$_1^{lox}$* allele and to exhibit germline competence were bred to 129S1 females. The resulting heterozygous offspring were interbred and genotyped by PCR or Southern blotting (Fig. 2, B–D). Note that the *Ly49q$_1$* probe also detects the closely related *Ly49q$_2$* and *q$_3$* pseudogenes of the 129 gene cluster, as all three genes display the same WT KpnI fragment (Fig. 2 B). However, mice heterozygous or homozygous for the *Ly49q$_1^{neo}$* or *Ly49q$_1^{lox}$* alleles are easily distinguished by PCR using *Ly49q$_1$*-specific primers that do not detect the *Ly49q$_2$* or *q$_3$* pseudogenes (Fig. 2, C and D).

The insertion of a *PGK-neo* cassette or *loxP* site into exon 2 did not eliminate transcription, as revealed by RT-PCR (unpublished data). Analysis of the targeted cDNA revealed that insertion of *PGK-neo* or *loxP* interrupted the open reading frame, leading to premature termination. Both pDCs and mDCs from *Ly49q$_1^{neo/neo}$* and *Ly49q$_1^{lox/lox}$* mice lack any detectable Ly49Q by flow cytometry (Fig. 2 E and not depicted). We have reported that, in addition to pDCs, neutrophils also express low levels of Ly49Q protein (10). *Ly49q$_1^{lox/lox}$* blood neutrophils lacked all detectable reactivity with anti-Ly49Q mAb (unpublished data), confirming that

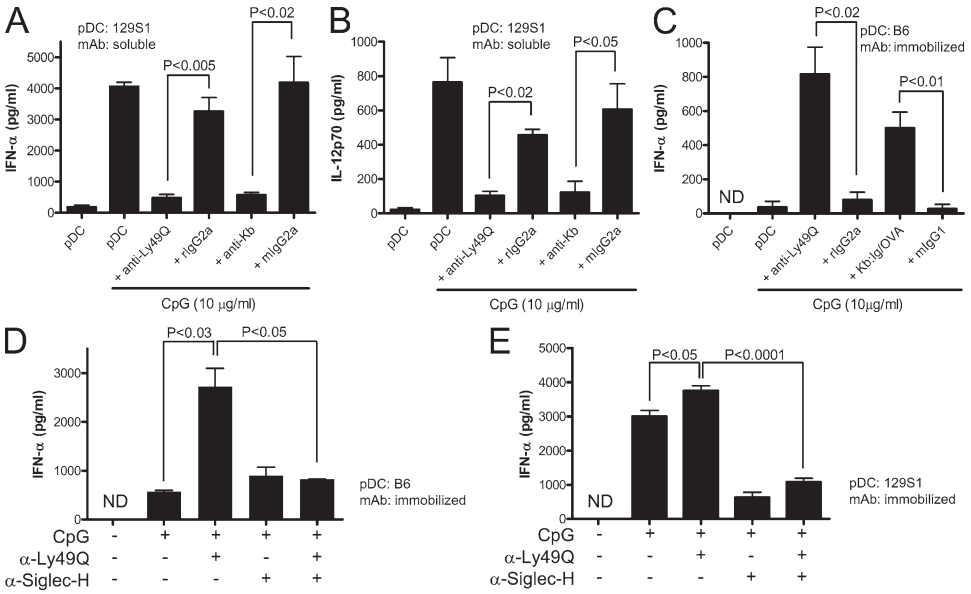

Figure 1. Ly49Q–H-2K^b interactions are necessary for pDC cytokine secretion after TLR9 stimulation. (A and B) Splenic pDCs from 129S1 mice were isolated using mPDCA-1 microbeads and cultured overnight in the presence or absence of CpG-ODN and the indicated mAb. The supernatant was assayed by ELISA for IFN-α (A) or IL-12p70 (B). (C–E) Splenic pDCs from B6 (C and D) or 129S1 (E) mice were isolated with mPDCA-1 microbeads and cultured overnight in wells that had been precoated with the indicated mAb or recombinant MHC molecule in the presence or absence of 10 μg/ml CpG. The supernatant was assayed by ELISA for IFN-α. Isotype control antibodies for anti-Ly49Q, anti–H-2K^b, and K^b:Ig/OVA are rIgG$_{2a}$, mIgG$_{2a}$, and mIgG$_1$, respectively. Anti-Ly49Q mAb 2E6 was used for these experiments. Data are presented as the mean of triplicate samples (error bars = SD). Results are representative of at least three independent experiments. ND, not detectable.

Ly49Q is normally expressed at low levels on this cell type. Collectively, these data demonstrate that the open reading frame of *Ly49q*$_1$ was disrupted successfully.

The effect of introducing *PGK-neo* or a *loxP* site in *Ly49q*$_1$ on neighboring gene expression was assessed by flow cytometry on both resting and IL-2–cultured NK cells with mAb recognizing proteins encoded by genes 5′ (*Ly49g*, *Ly49r*, and *Ly49e/s*) and 3′ (*Nkg2a/c/e* and *Nkg2d*) of *Ly49q*$_1$. Both the distribution and lmean fluorescence intensity (MFI) of these receptors were the same on *Ly49q*$^{wt/wt}$, *Ly49q*$^{neo/neo}$, and *Ly49q*$^{lox/lox}$ NK cells (unpublished data). This indicates that the targeted insertion had no secondary effect on other genes located within the natural killer gene complex. Furthermore, Ly49Q-null pDC H-2K^b and H-2D^b surface levels were identical to those of Ly49Q-WT pDCs (unpublished data). As *Ly49q*$_2$ and *q*$_3$ are likely pseudogenes, *Ly49q*$_1$ will be referred to as *Ly49q* hereafter. Unless otherwise stated, all experiments were performed with *Ly49q*$^{wt/wt}$ (WT) or *Ly49q*$^{lox/lox}$ (Ly49Q-null) littermates in the high IFN-producing 129 background.

Hematopoiesis and pDC development in Ly49Q-null mice

Fresh splenic pDCs are round cells with eccentric kidney-shaped nuclei, as visualized by Giemsa stain (Fig. 3 A). After activation with CpG-ODN, pDCs were larger and displayed a higher cytoplasmic to nucleus content, and the cytoplasm also appeared more vacuolated. The size and morphology of resting or activated pDCs from Ly49Q-WT and -null mice were similar. To determine whether the localization of Ly49Q-null

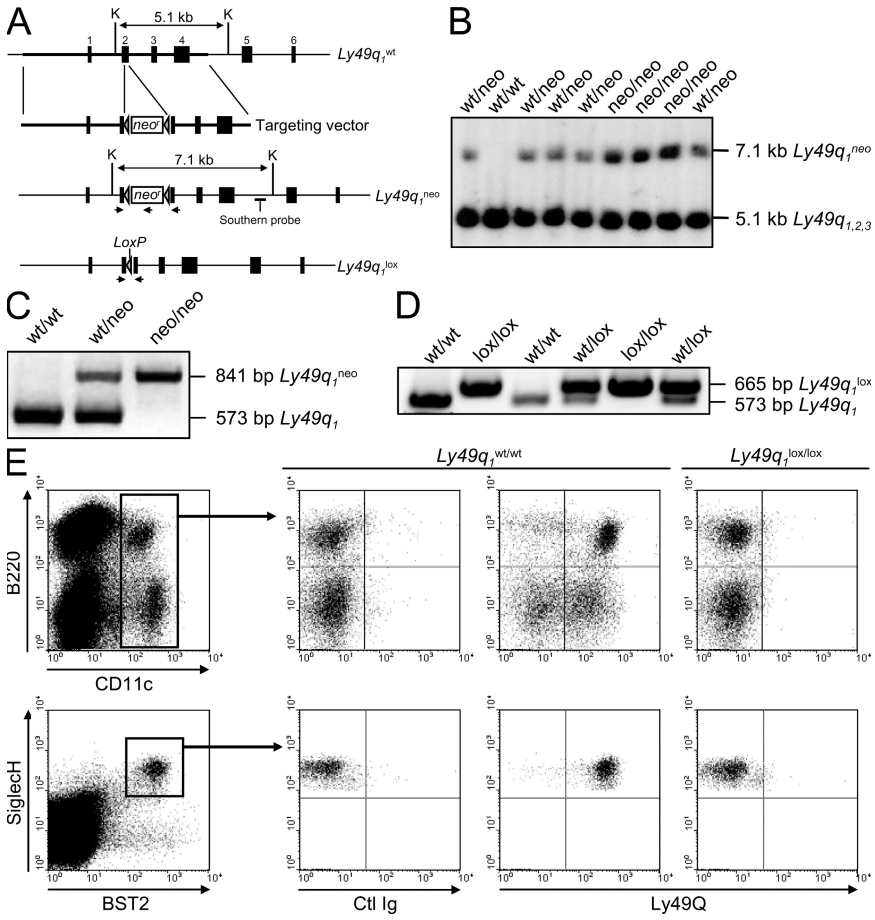

Figure 2. Generation of Ly49Q-null mice. (A) *Ly49q*$_1$ gene disruption strategy. A 10-kb segment encompassing exons 1–4 was cloned by recombineering from BAC DNA, and a floxed *PGK-Neo*^{r} (*neo*^{r}) cassette was inserted into exon 2. After electroporation and selection, an ES clone possessing the predicted KpnI (K) fragment, as verified by Southern blotting, was electroporated with CMV-Cre plasmid, and the deletion of *PGK-Neo*^{r} was confirmed by PCR. Both *Ly49q*$_1^{neo}$ and *Ly49q*$_1^{lox}$ mice were created. PCR primers are shown by arrowheads. Boxes denote exons, and the location of the Southern probe is underlined. (B) Southern blot analysis. Genomic tail DNA of pups from *Ly49q*$_1^{neo/wt}$ parent mice was digested with KpnI and analyzed by Southern blotting with the probe depicted in A. Note that the probe detects identical fragments from *Ly49q*$_1$, *q*$_2$, and *q*$_3$ genes. (C) PCR analysis of tail DNA from mice in B. To eliminate confusion caused by *Ly49q*$_2$ and *q*$_3$ genes, *Ly49q*$_1$-specific primers were designed. These primers were used to analyze tail DNA by PCR and to differentiate between *Ly49q*$_1^{wt}$ and *Ly49q*$_1^{neo}$ alleles. (D) PCR analysis of pups from *Ly49q*$_1^{lox/wt}$ parent mice. Tail DNA was PCR amplified with primers flanking exon 2 to differentiate *Ly49q*$_1^{wt}$ and *Ly49q*$_1^{lox}$ alleles. (E) Lack of Ly49Q protein on DCs derived from Ly49Q-null mice. Ly49Q-null and -WT splenocytes were stained with a combination of mAb to CD11c/B220 (top) or Siglec-H/BST2 (bottom), and Ly49Q-specific mAb NS-34 or an isotype control. Ly49Q mAb staining intensity relative to isotype control mAb on gated cells is shown.

pDCs is normal, three-color immunofluorescent staining using mPDCA-1, CD3, and CD19 mAbs was performed on splenic sections from untreated and CpG-ODN–treated animals. In the spleens of untreated animals, pDCs were mainly localized within the T cell zones and in lower numbers within marginal zone and red pulp (Fig. 3 B). In CpG-ODN–treated animals, the number of pDCs was increased and they tended to form clusters (Fig. 3 B). The majority of CpG-activated pDCs were found within the marginal zone and red pulp, as previously reported (23). Thus, no significant differences were observed in the localization of pDCs in WT and Ly49Q-null mice before or after CpG-ODN treatment.

The potential effect of Ly49Q absence on pDC frequency and distribution of cells in primary and secondary lymphoid organs was investigated in the Ly49Q-null mice. The pDC population as defined by $CD11c^+Siglec\text{-}H^+$ showed no significant difference in the proportion and total number of pDCs in the spleen, mesenteric lymph nodes, or bone marrow of young mice (6 wk old; Fig. 3 C and not depicted). However, in older mice (>9 mo old) there was approximately a twofold increase in the proportion and total number of pDCs in these organs (Fig. 3 C and not depicted). Myeloid lineage cells in various organs have been reported to express Ly49Q. There were no significant differences in the percentage and total number of $CD11b^+Gr\text{-}1^+$ cells in the bone marrow, spleen, or lymph nodes in either young or old mice (unpublished data). Similarly, blood neutrophil numbers and proportion in WT mice and Ly49Q-null littermates were not significantly different (unpublished data). In fact, no significant difference for any lineage tested was observed, including the B, NK, NKT, $CD4^+$ T, or $CD8^+$ T cells, or mDC subsets in either young or old mice (unpublished data). Therefore, Ly49Q deficiency appears to selectively affect pDC development and homeostasis, albeit only modestly. Young mice (5–8 wk old) were chosen for all functional experiments.

Severe defect in TLR9-induced IFN-α production by Ly49Q-null pDCs

To determine the effect of Ly49Q deficiency on pDC activation and subsequent cytokine production, the response of Ly49Q-null pDCs to TLR9 agonists was evaluated. Splenic pDCs were isolated from WT and Ly49Q-null littermates using mPDCA-1–conjugated magnetic beads, cultured overnight in various concentrations of CpG-ODN, and the supernatant was assayed for IFN-α. Remarkably, Ly49Q-null pDC supernatants yielded approximately fivefold lower levels of IFN-α relative to supernatants from identically treated WT pDCs (Fig. 4 A). This finding is consistent with the earlier observation that Ly49Q binding to $H\text{-}2K^b$ is necessary for TLR9-mediated IFN-α secretion (Fig. 1 A). In parallel, Ly49Q-deficient pDCs showed a significant defect in IL-12 secretion in response to CpG-ODN compared with WT pDCs (Fig. 4 B). The IL-12 defect was not as pronounced as that observed for IFN-α but is consistent with the decrease in IL-12 production observed upon mAb-mediated blockade of Ly49Q–$H\text{-}2K^b$ interactions (Fig. 1 B). In contrast, TNF-α and IL-6

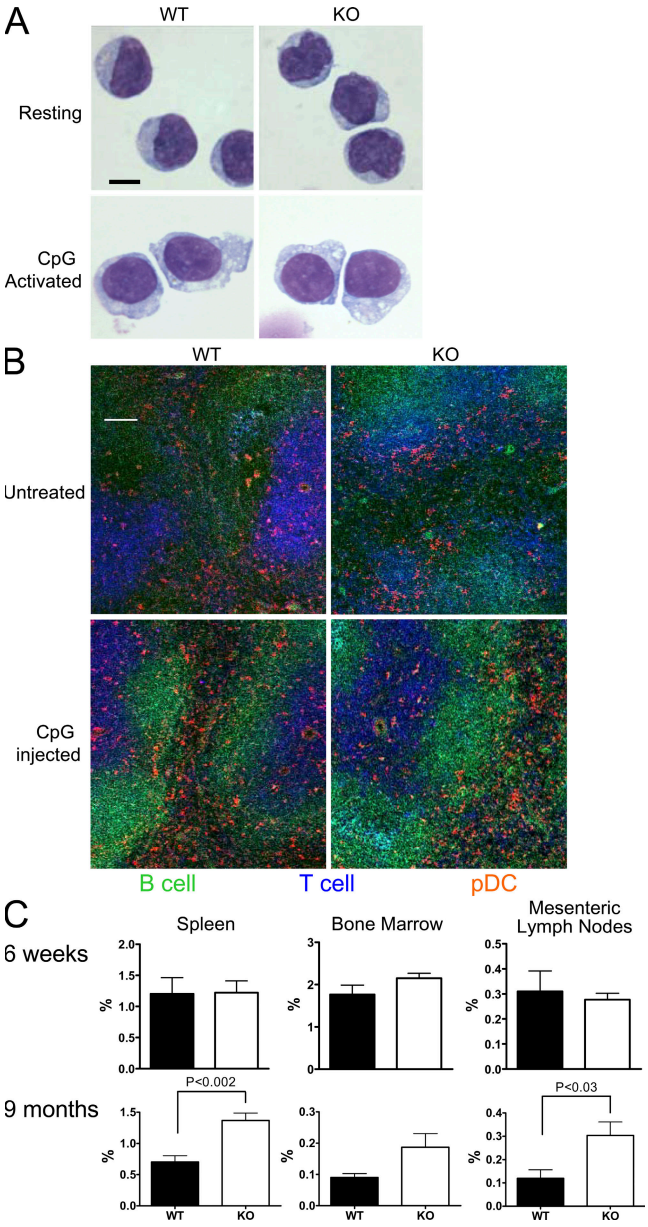

Figure 3. Age-dependent increase in pDC proportion in Ly49Q-null mice. (A) pDC size and morphology. pDCs were sorted as $CD11c^+B220^+CD11b^-DX5^-CD3^-CD19^-$ cells from the spleen and cytocentrifuged on microspcope slides directly as resting pDCs or after incubation with 3 µg/ml CpG for 16 h. Slides were then stained with Giemsa solution. Bar, 5 µm. (B) Localization of splenic pDCs. Sections of spleen isolated from untreated young mice or mice injected i.v. with 10 µg/ml CpG 24 h earlier were stained with fluorescently labeled mAb to CD19 (B cells; green), CD3 (T cells; blue), and BST2 (pDCs; red). Bar, 50 µm. (C) Frequency of pDCs in primary and secondary lymphoid organs. Shown are the proportion of pDCs defined as $CD11c^+Siglec\text{-}H^+$ cells in lymphoid organs of $Ly49q^{+/+}$ (closed bars) and $Ly49q^{lox/lox}$ (open bars) mice (6 wk old, $n = 3$; 9 mo old, $n = 6$). A similar pattern was observed with BST2 staining (not depicted). Data are presented as the mean of individual mice (error bars = SD). Results are representative of at least three independent experiments, except for C (9-mo-old mice), which was done twice.

production were not compomised in Ly49Q-deficient pDCs (Fig. 4, C and D). Thus, Ly49Q-deficient pDCs possess an intrinsic defect in IFN-α production after stimulation with TLR9 agonists in vitro.

Injection of mice with CpG-ODN leads to a rapid elevation of serum IFN-α peaking at 6 h after treatment that is mediated by pDCs (23). To determine whether the in vitro cytokine defect of Ly49Q-null pDCs had in vivo consequences, mice were injected with CpG-ODN, and serum IFN-α levels were evaluated after 6 h. Importantly, IFN-α serum levels in CpG-injected Ly49Q-null mice were consistently 5–10-fold less than those of WT littermates (Fig. 4 E). On the other hand, the sera of both cohorts showed similar levels of IL-12 (unpublished data). The normal serum IL-12 levels detected in Ly49Q-null mice after CpG injection were most likely caused by TLR9-mediated IL-12 production by cell types other than pDCs (24). A time-course experiment monitoring serum IFN-α levels confirmed that although maximal IFN-α levels occur 4–6 h after injection in WT mice, Ly49Q-null mice failed to attain a similar magnitude of IFN-α levels at any time point assayed (Fig. 4 F). Thus, Ly49Q-null mice display an inherent defect in IFN-α

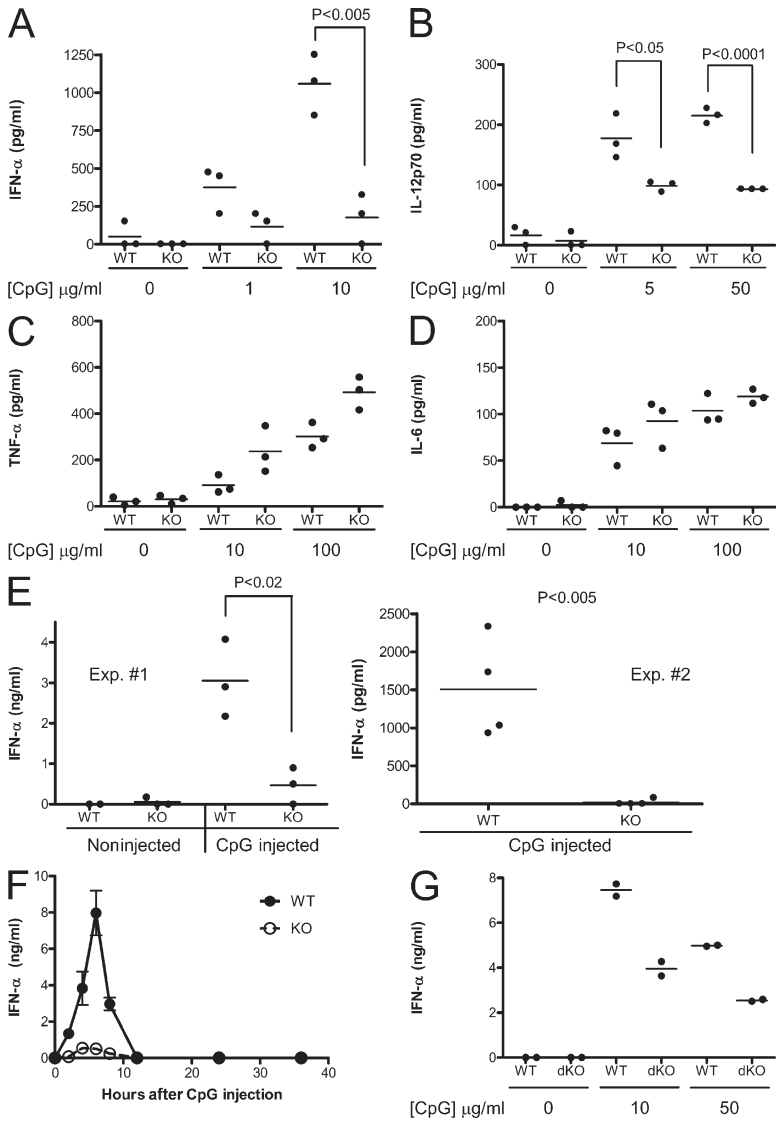

Figure 4. Ly49Q-null pDCs display an IFN-α production defect in response to CpG-ODN. (A–D) IFN-α production by isolated pDCs after CpG-ODN stimulation. pDCs were isolated with mPDCA-1 microbeads from Ly49Q-null and -WT mice and cultured overnight in the presence of the indicated concentrations of CpG-ODN. Culture supernatants were assayed by ELISA for IFN-α (A), IL-12p70 (B), TNF-α (C), or IL-6 (D). (E) Induction of serum cytokines by CpG-ODN injection. Ly49Q-null and -WT littermates were injected with CpG-ODN + DOTAP, and blood samples were taken after 6 h for IFN-α ELISA. Uninjected mice served as controls. Each symbol represents a single mouse. (F) Serum IFN-α time course after CpG-ODN stimulation. Ly49Q-null and -WT littermates were injected with CpG-ODN + DOTAP, and blood was collected periodically over 36 h. Serum IFN-α levels were deduced by ELISA from three mice of each genotype for each time point. Data are representative of experiments done at least three times independently (error bars = SD). (G) pDCs were isolated from H-2K^{b}D^b–null or –WT (B6) mice and treated as in A. Horizontal bars represent means.

production in vivo, and IFN-α and IL-12 responses to CpG-ODN can be uncoupled in these mice. Although the absence of the receptor leads to clear defects in cytokine production, the effect of loss of the ligand is unknown. Thus, pDCs were isolated from H-2K^{b}D^b–null mice and were stimulated for IFN-α production by CpG-ODN. H-2K^{b}D^b–null pDCs showed ∼50% reduction in IFN-α secretion compared with WT pDCs (Fig. 4 G). These results are consistent with the hypothesis that Ly49Q–MHC interactions are necessary for cytokine production in pDCs, whereas the inhibition of IFN-α secretion was not as pronounced as for Ly49Q-null pDCs. Possible reasons for this difference may include the mouse strain background or that Ly49Q may have other ligands in addition to H-2K^b.

To address the question of whether Ly49Q/MHC interact in cis or trans to regulate pDC function, Ly49Q-null mice were crossed to H-2K^{b}D^b–null mice, and the resulting F1 mice were intercrossed to generate the four possible null phenotypes. pDCs from WT mice stain positively with soluble H-2K^b/OVA tetramer, and this binding is caused by Ly49Q, as shown by the complete absence of binding in Ly49Q-null mice and by previous blocking experiments with anti-Ly49Q mAb (Fig. 5 A, compare the top two dotplots) (21). In the absence of H-2K^b expression, binding of the H-2K^b tetramer is much stronger but still Ly49Q dependent (Fig. 5 A, compare the bottom two dotplots). Differential tetramer binding was not caused by differences in Ly49Q expression between WT and H-2K^{b}D^b–null mice, as pDCs from both mouse strains expressed similar levels of Ly49Q (Fig. 5 B). These results suggest that in WT pDCs, cis interactions between Ly49Q and endogenous H-2K^b are inhibiting binding of soluble H-2K^b tetramer to Ly49Q.

Normal TLR9 expression and pDC activation in Ly49Q-deficient mice

Although the in vitro mAb-mediated blocking experiments are consistent with the phenotype of Ly49Q-null pDCs in vitro and in vivo, the defect in TLR9-induced cytokine production might be the result of factors other than the absence of Ly49Q. First, Ly49Q deficiency may have caused down-regulation of TLR9. To exclude this possibility, TLR9 expression was determined by RT-PCR and intracellular flow cytometry given the localization of TLR9 in endosomes. TLR9 levels were measured and found to be similar in both Ly49Q-WT and -null pDCs (Fig. 6 A and not depicted), suggesting that Ly49Q-null pDCs have an equal potential to bind CpG-ODN. Second, the almost complete lack of IFN-α secretion by Ly49Q-null pDCs may be caused by an inability of the cells to become fully activated. Downstream activation events in pDCs both in vivo (Fig. 6 B) and in vitro (Fig. 6 C) after CpG-ODN challenge were assessed by flow cytometry analysis of CD86 and class II MHC surface expression, and were found to be normal. The percentage of pDCs expressing CD86 and the level of CD86 on pDCs were similar between WT and Ly49Q-null pDCs after CpG treatment, even over an extended range of doses (Fig. 6, B and C). Similar observations were made for class II MHC (unpublished data). Collectively, these data suggest that the signaling pathways downstream of TLR9 that induce expression of CD86/class II MHC are different from those that lead to IFN-α production such that Ly49Q signaling modulates only the latter responses in pDCs.

TLR7-mediated cytokine secretion is defective in Ly49Q-null mice

To further characterize the extent of the defect in Ly49Q-null pDC cytokine responses, a distinct TLR pathway was evaluated. In addition to high levels of TLR9, pDCs also express TLR7, which can recognize single-stranded RNA motifs represented by such viruses as influenza and vesicular stomatitis virus. Similar to CpG-ODN stimulation, infection of isolated pDCs with influenza virus resulted in high levels of secreted IFN-α, as previously reported (6). Ly49Q-null pDCs produced fivefold less IFN-α and threefold less IL-12 than WT pDCs in response to influenza (Fig. 7, A and B).

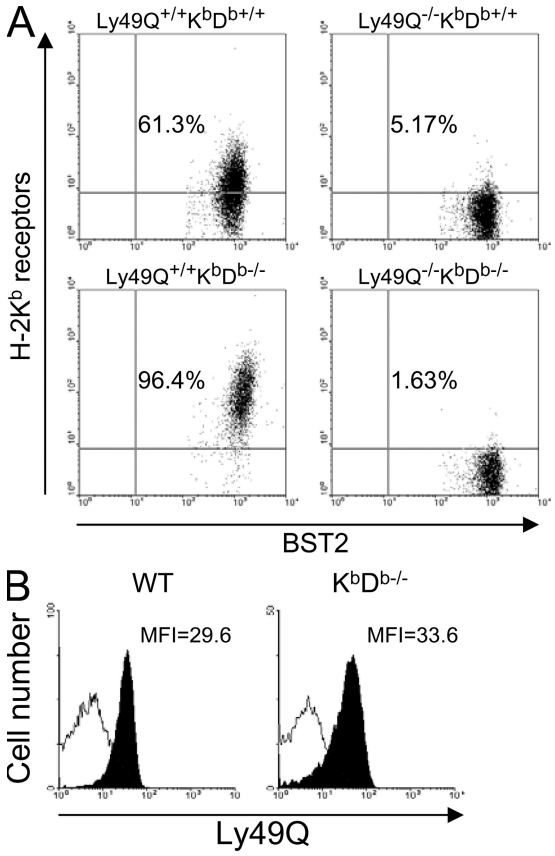

Figure 5. Ly49Q binds to H-2K^b in cis. (A) pDCs were isolated from the spleens of mice with the indicated genotypes with mPDCA-1 microbeads. Isolated pDCs were stained with PE–H-2K^b/OVA tetramer and allophycocyanin–anti-BST2 mAb and were analyzed by flow cytometry. Cells are gated on pDCs. The percentage of cells positively staining with PE–H-2K^b/OVA is shown. (B) Ly49Q levels on MHC-deficient pDCs. Splenocytes from the indicated strains (WT is B6) were stained for BST2, Siglec-H, and Ly49Q (NS34). The level of Ly49Q expression on BST2$^+$Siglec-H$^+$ cells is shown (shaded histogram). The open histogram represents the secondary reagent alone.

Active and inactivated influenza virus treatments gave similar results (unpublished data). In contrast, CD86 and class II MHC up-regulation of isolated pDCs in response to a TLR7 agonist was normal in Ly49Q-null pDCs (Fig. 7 C and not depicted). Therefore, TLR7-induced cytokine secretion is also attenuated in Ly49Q-null pDCs.

Ly49Q-deficient mice exhibit diminished protection to mouse CMV (MCMV) infection

The defect in IFN-α production seen in Ly49Q-null mice after TLR9 stimulation may have deleterious consequences during immune responses against pathogens that are detected through TLR9. Previous studies have reported that TLR9 deficiency promotes increased susceptibility to MCMV infection, as manifested by higher viral loads and defective production of multiple cytokines, including type I IFN (24, 25). As such, the defect in TLR9-dependent IFN-α production observed in Ly49Q-null mice may also lead to diminished pDC responses and altered innate immunity to DNA viruses like MCMV. In keeping with this, purified Ly49Q-null pDCs produce approximately threefold less IFN-α than WT pDCs in response to overnight MCMV infection in vitro (Fig. 8 A). The MCMV/pDC co-culture experiment confirms, independently of CpG-ODN, that pDCs from Ly49Q-null mice display defective IFN-α production when triggered through TLR9.

To confirm these findings in vivo, Ly49Q-null mice were infected with MCMV. As shown in Fig. 8 B, splenic viral titers were consistently higher in Ly49Q-null mice versus WT control animals. Although not all experiments showed a statistically significant difference between the two cohorts (e.g., day 3, 6,000 PFU; Fig. 8 B), the detection of impaired viral immunity may be complicated by the susceptible Ly49H$^-$ 129 background of these mice (26). Because

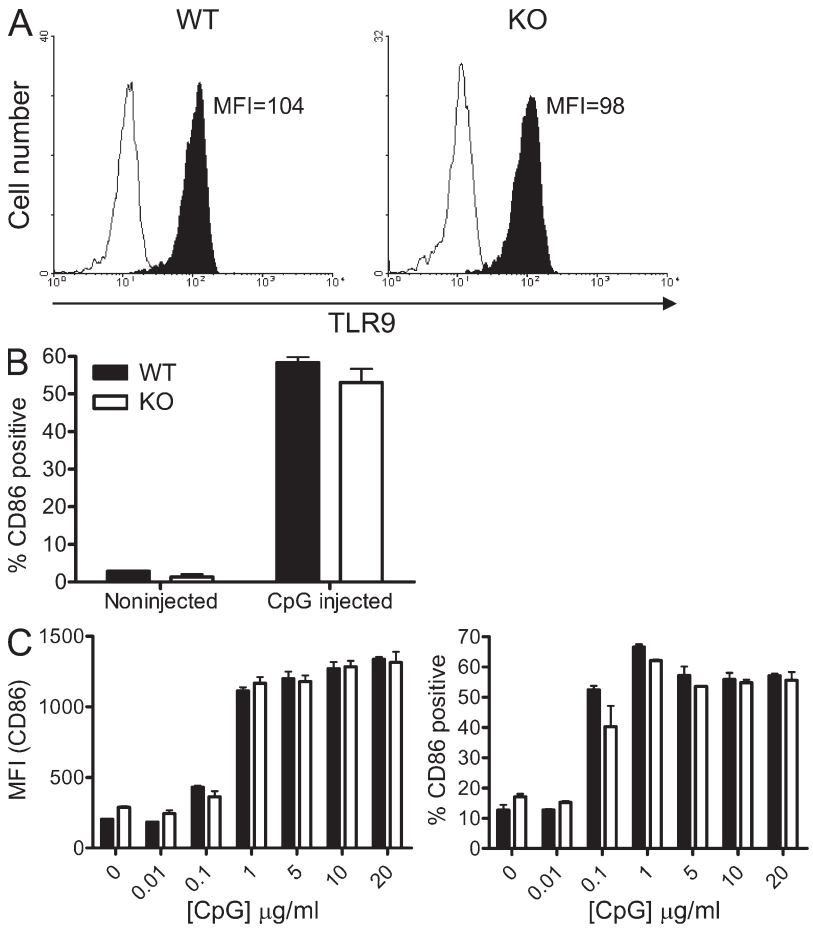

Figure 6. Normal TLR9 and CD86 expression by Ly49Q-null pDCs. (A) Splenocytes from Ly49Q-null and -WT mice were stained for Siglec-H and BST2, and were then permeabilized and stained for intracellular TLR9 or with an isotype control mAb. TLR9 (shaded histogram) or control (open histogram) expression on Siglec-H$^+$BST2$^+$ cells is shown. (B) In vivo activation of pDCs by CpG-ODN. Ly49Q-null and -WT littermates were injected with CpG-ODN + DOTAP. Uninjected mice served as controls. After 6 h, the splenocytes were isolated and stained for Siglec-H, BST2, and CD86, and were analyzed by flow cytometry. The percentage of CD86$^+$ pDCs after 6 h is shown (error bars = SD). (C) In vitro activation of pDCs by CpG-ODN. pDCs from Ly49Q-null and -WT mice were isolated with mPDCA-1 microbeads and cultured overnight in the presence of the indicated concentrations of CpG-ODN. The following day, the CD11c$^+$B220$^+$ cells were analyzed by flow cytometry for CD86 surface expression. MFI (left) and the percentage of positive cells (right) are shown as the means of triplicate cultures ± SD. Data are representative of at least three independent experiments.

the *Ly49h* gene conferring resistance to MCMV in B6 mice (27, 28) is <300 kb away from the targeted $Ly49q^{lox}$ allele, these experiments could not be repeated on the MCMV-resistant B6 background at this time. Notwithstanding this, the majority of experiments did reveal a statistically significant increase in Ly49Q-null MCMV titers when performed using either an early time point (1.5 d after infection) or a low initial MCMV inoculum (600 PFU), or both (Fig. 8 B). In agreement with our findings, TLR9-null mice on a susceptible background ($Ly49H^-$ BALB/c) display a similarly small but significant increase in splenic viral titers after MCMV infection (24). Serum IFN-α and IL-12 levels peak at 36 h after MCMV infection. At this time point, Ly49Q-null mice display normal levels of IFN-α (Fig. 8 C) and slightly decreased IL-12p70 levels (Fig. 8 D). This suggests that in addition to pDCs, other cell types can contribute to serum IFN-α/IL-12 levels by 36 h after infection. Collectively, these experiments demonstrate that Ly49Q-null pDCs exhibit a functional deficiency in IFN-α production in response to MCMV infection in vitro, and this translates into an enhanced susceptibility of Ly49Q-null mice to MCMV infection in vivo.

DISCUSSION

Ly49q is a highly conserved *Ly49* found in all mouse strains characterized to date (16). Ly49Q is also unique in being expressed on pDCs, in contrast to all other Ly49s. We have previously shown, using the BWZ lacZ-based reporter cell assay, that H-$2K^b$ is a high affinity ligand for Ly49Q (21). In this study, we confirm the specificity of Ly49Q for H-$2K^b$ in a functional assay (IFN-α secretion) using fresh ex-vivo pDCs. Remarkably, Ly49Q–H-$2K^b$ interactions appear to be required for optimal TLR7- and TLR9-dependent stimulation of cytokine production by pDCs, as indicated by the drastic reduction in CpG-mediated IFN-α and IL-12 secretion upon mAb-mediated blockade of either Ly49Q receptor or its cognate ligand, H-$2K^b$. In further support of this

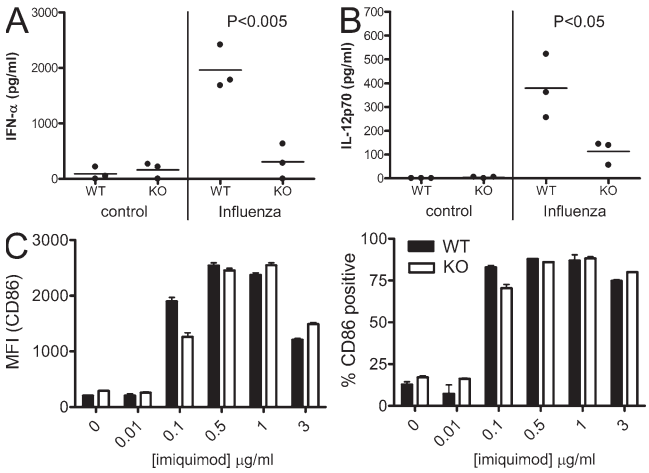

Figure 7. TLR7-induced cytokine production is defective in Ly49Q-null pDCs. (A and B) In vitro activation of pDCs by influenza virus. pDCs from Ly49Q-null and -WT mice were isolated using mPDCA-1 microbeads and cultured overnight in the presence or absence of 20 hemagglutinin units of influenza virus. Culture supernatants were assayed by ELISA for IFN-α (A) or IL-12p70 (B). Each symbol represents a single mouse. Horizontal bars represent means. (C) In vitro activation of pDCs by imiquimod. pDCs from Ly49Q-null and -WT mice were isolated using mPDCA-1 microbeads and cultured overnight with the indicated concentrations of imiquimod. The following day, $CD11c^+B220^+$ cells were stained with FITC–anti-CD86 and analyzed by flow cytometry for CD86 surface expression. MFI (left) and the percentage of positive cells (right) are shown as the means of triplicate cultures ± SD. Data are representative of at least three independent experiments.

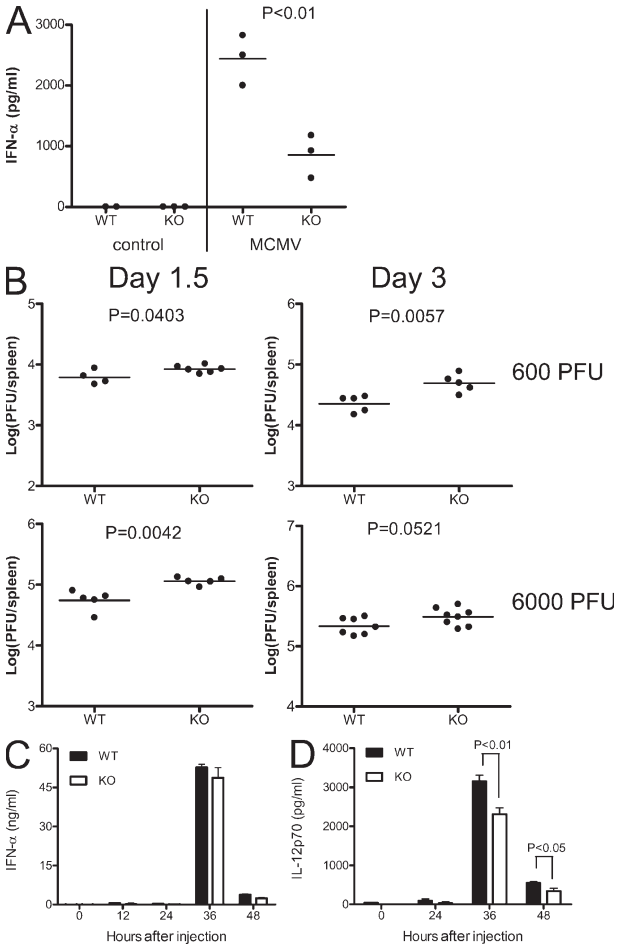

Figure 8. Reduced anti-MCMV responses by Ly49Q-null mice. (A) Decreased MCMV-induced IFN-α secretion by pDCs in vitro. Splenic pDCs were isolated with mPDCA-1 microbeads and cultured overnight in the presence of 200 PFU/ml of MCMV. Supernatants were harvested the following day. Supernatants were assayed for IFN-α levels by ELISA. (B) Greater MCMV proliferation in Ly49Q-null mice. Ly49Q-null and -WT mice were challenged with 600 or 6,000 PFU MCMV. After 1.5 or 3 d, spleens were harvested and viral titer was determined using BALB/c mouse embryo fibroblasts. Each symbol represents a single mouse. Data are representative of at least three independent experiments. Horizontal bars represent means. (C and D) Littermates of the indicated genotypes were infected with 6,000 PFU MCMV i.p., and serum samples were taken at the indicated time points after infection. IFN-α (C) or IL-12p70 (D) levels were determined by ELISA ($n = 4$ per time point). The means of individual mice ± SD are shown.

hypothesis, purified pDCs cultured in the presence of low concentrations of CpG-ODN produced high levels of IFN-α when stimulated on immobilized Ly49Q mAb or H-2K^b/Ig fusion protein but not in the presence of CpG-ODN alone. Collectively, these findings demonstrate that Ly49Q–class I MHC interactions positively regulate TLR signals and subsequent cytokine production in pDCs.

In confirmation of the in vitro mAb blocking experiments, Ly49Q-null mice show a severe defect in systemic IFN-α levels (75–100% reduction) upon challenge with CpG-ODN. This defect is likely caused by the hyporesponsiveness of Ly49Q-null pDCs, as purified pDCs from these mice exhibit similarly decreased IFN-α responses upon CpG-mediated stimulation in isolation. Ly49Q-null pDCs also show a defect in the production of IFN-α after overnight culture with MCMV. Both CpG-ODN and MCMV stimulate IFN-α production by pDCs in a TLR9-dependent manner (24). However, TLR9 mRNA and protein expression levels in Ly49Q-null pDCs are normal, as deduced by semiquantitative RT-PCR and intracellular staining, respectively. The Ly49Q-null defect similarly affects TLR7, as TLR7-dependent stimulation of isolated Ly49Q-null pDCs results in highly decreased levels of IFN-α relative to WT pDCs. Notably, in addition to IFN-α levels, Ly49Q-null pDCs also exhibit decreased IL-12p70 levels in response to CpG-ODN or influenza stimulation. Thus, Ly49Q-null pDCs possess an intrinsic cytokine production defect in response to TLR7 and TLR9 agonists. Interestingly, however, the activation status of Ly49Q-null pDCs seems normal over a wide range of CpG-ODN concentrations, at least with respect to up-regulation of CD86 and class II MHC surface expression, TNF-α and IL-6 production, morphological change, and migration within the spleen. This suggests that TLR9 stimulation results in multiple signaling pathways leading to pDC activation, but that Ly49Q regulates only the signal transduction pathway leading to IFN-α secretion.

The phenotype of pDCs from Ly49Q-null mice is similar to that observed for Ly49Q-negative pDCs from WT bone marrow. Omatsu et al. found that Ly49Q-negative pDCs produced significantly less IFN-α/β than their Ly49Q-positive counterparts when cultured in the presence of CpG-ODN or Sendai virus (19). In contrast, Kamogawa-Schifter et al. observed comparable IFN-α production levels from the two pDC subsets in vitro after stimulation with CpG-ODN (11). It is not immediately clear why there is a discrepancy in IFN-α production among Ly49Q-positive versus -negative pDCs in these two studies, as similar isolation procedures and the same mouse strain (BALB/c) were used. The data presented in this paper agree with the former study, in that the ability of pDCs to produce large amounts of IFN-α appears to depend on Ly49Q expression and function.

The positive regulation of TLR9 signaling by Ly49Q is at first counterintuitive, given that the ITIM-bearing Ly49Q receptor has the characteristics of an inhibitory Ly49 family member. Similar Ly49 receptors expressed by NK cells undergo tyrosine phosphorylation of their cytoplasmic ITIM in response to receptor engagement, resulting in the recruitment of SHP-1/2 (29). Ly49-associated SHP-1/2 are then thought to antagonize stimulatory signals initiated through ITAM-bearing adaptor molecules such as DAP12. For example, the ITIM-bearing Ly49G receptor has been demonstrated to suppress DAP12-dependent Ly49D-mediated cytotoxicity and cytokine production (30). Notably, the ability of the Ly49Q ITIM to associate with SHP-1/2 is intact, at least in reconstitution experiments using transfected cell lines (10). Thus, if Ly49Q is an inhibitory receptor, how does it function to relay TLR7/9-induced signals or amplify TLR7/9-mediated signal transduction? Interestingly, there are clues from experiments performed using DAP12-null mice that may offer a possible mechanism. Specifically, DAP12-null pDCs were reported to produce significantly more IFN-α after CpG-ODN stimulation (31), as opposed to the decreased response of Ly49Q-null mice. The resulting conclusion was that DAP12 may negatively regulate TLR7/9 signal transduction and, in turn, that DAP12-coupled receptors on pDCs may inhibit IFN-α secretion upon cross-linking. In support of this hypothesis, the pDC-expressed and DAP12-associated surface proteins Nkp44 and Siglec-H do indeed inhibit CpG-induced IFN-α secretion upon mAb-mediated ligation (12, 22). In this respect, macrophages and pDCs are functionally similar, as macrophages from DAP12-null mice produce more cytokines after TLR engagement (32). Furthermore, the DAP12-coupled TREM2 surface receptor appears to deliver constitutive inhibitory signals in macrophages (33).

The apparent stimulatory role of Ly49Q in pDCs could be caused by antagonism of inhibitory DAP12 signal transduction by SHP-1/2 recruited as a result of Ly49Q–MHC interaction. In this model, DAP12 signaling would be constitutive like TREM2 function in macrophages (33). Although the convergence point between the DAP12 and TLR9 signaling pathways is unclear, another possibility is that downstream Ly49Q signaling molecules may directly regulate the TLR9 signaling cascade independently of DAP12 function. A third mechanism behind Ly49Q function may include an alternative signaling pathway found in pDCs, one which is distinct from canonical inhibitory Ly49 signaling in NK cells and does not involve the recruitment of tyrosine phosphatases. Evidence for this possibility includes Ly49Q-transfected macrophage cell lines, which show an increase in tyrosine-phosphorylated proteins in whole-cell lysates after mAb-mediated cross-linking of Ly49Q (10).

The mechanistic link between Ly49Q function and IFN-α secretion is unknown. However, an interesting parallel may exist between NK cells and pDCs in this regard. Two reports have suggested that mature splenic NK cells lacking all self-specific MHC-binding inhibitory receptors (NKG2A and Ly49C/I in B6 mice) are hyporesponsive with respect to the killing of target cells and the production of IFN-γ (34, 35). Thus, B6 strain NK cells expressing NKG2A and/or Ly49C/I have been referred to as being "licensed" or "armed." It is tempting to speculate that pDCs like NK cells may also require the expression of at least one self-specific MHC-binding

inhibitory receptor to become fully functional IFN-α producers. This hypothesis is consistent with the hyporesponsiveness observed for immature Ly49Q-negative pDCs (19). Because Ly49Q binds with high affinity to H-2K^b, a self-specific determinant expressed in 129 strain Ly49Q-null mice, the lack of a self-MHC–specific inhibitory signal during pDC development in Ly49Q-null mice may render these cells anergic. However, the recapitulated phenotype using WT pDCs in mAb blocking experiments (Fig. 1) argues against Ly49Q-null pDCs being anergic.

Type I IFN is indispensable for resistance to a wide range of viruses, as shown by studies using IFN-α/βR-null mice (36). Ly49Q-null mice, which are on the Ly49H$^-$ 129 background, also display a severe IFN production defect, as well as a consistent and statistically significant increase in susceptibility to MCMV. However, the susceptibility of Ly49Q-null mice to virus infection is not as profound as that observed in IFN-α/βR-null mice. There are several possible reasons for this observation. First, although the magnitude of the IFN-α response to CpG-ODN challenge in WT mice far exceeds that of Ly49Q-null mice, the latter still yield up to 15–25% of WT serum IFN-α levels. This lower yet detectable IFN-α production may be sufficient to mount resistance to viral infection. This hypothesis is consistent with the phenotype of Ly49H$^+$ B6 mice, which produce low levels of IFN-α (6) but are nonetheless sufficient for protection against MCMV and other viruses. In agreement with our study, TLR9-null mice on a BALB/c (MCMV susceptible; Ly49H$^-$) background also only show a small increase in susceptibility (24), as would be expected if Ly49Q does indeed regulate TLR signaling. Furthermore, normal systemic IFN-α levels were observed in Ly49Q-null mice 36 h after MCMV infection despite their defective IFN-α responses to synthetic CpG-ODN. Therefore, although pDC cytokine production is compromised in Ly49Q-deficient mice and does confer limited susceptibility to viral infection, the residual capacity of these mice to produce antiviral cytokines probably affords sufficient protection. Whether these residual cytokines are made by Ly49Q-null pDCs or other cell types is not clear.

Based on the data generated from mAb-mediated blocking assays and functional analyses of Ly49Q-null pDCs in vitro, as well as in vivo analyses of Ly49Q-null mice, we conclude that pDC function, in particular IFN-α secretion, is regulated by class I MHC. The ability of pDCs to recognize class I MHC molecules is imparted by the lectin-like Ly49Q receptor, which in turn potentiates the capacity of pDCs to produce cytokines in response to TLR7 and TLR9 agonists. Loss of this self-recognition mechanism results in severe defects in IFN-α and IL-12 production by pDCs. Thus, Ly49Q–MHC interactions positively regulate pDC cytokine production triggered through TLR. Therefore, the down-regulation of class I MHC by certain viruses like MCMV could also result in the attenuation of pDC antiviral defense mechanisms in addition to evasion of CD8$^+$ T cell responses. Interestingly, despite bearing a consensus ITIM sequence, the function of Ly49Q on pDCs appears to be stimulatory in nature. Although this is somewhat paradoxical, it is nonetheless consistent with the reported counterregulatory function of DAP12-coupled receptors in pDCs, which appear to be inhibitory.

MATERIALS AND METHODS

Mice. 129S1 and B6 mice were purchased from the Jackson Laboratory. *H-2Kb^{tm1}H-2Db^{tm1}* (K^{b}D^b-KO) mice on a B6 background were purchased from Taconic. Mice were maintained and bred in the Clinical Research Institute of Montréal (IRCM) specific pathogen-free animal facilities. All manipulations performed on animals were in accordance with IRCM guidelines and were approved by the IRCM Animal Ethics Committee. Unless otherwise mentioned, all mice used for experiments were 5–8 wk of age.

Generation of Ly49Q-null mice. We previously identified 129S6 bacterial artificial chromosome (BAC) clones containing *Ly49q$_1$* (15). A 10-kb segment centered on exon 2 was retrieved from BAC 34o6 into the pMCIT-KpANhe vector by lambda red–mediated recombineering in EL350 cells, as previously described (37). To complete the targeting construct, a floxed PGK-neomycin cassette from PL400 was inserted into a unique StuI site in exon 2. The complete targeting construct sequence was confirmed. R1 ES cells (129Sv × 129Sv-CP) were electroporated with NotI-linearized targeting vector DNA and were then selected in G418. Homologous recombination in ES cells was assessed by Southern blotting. A homologous recombination efficiency of 1% was observed (6 out of 600). The germline competency of these clones was confirmed by generating heterozygous founder mice, which were then bred to achieve Ly49Q$^{neo/neo}$ homozygosity. An ES clone carrying a properly targeted *Ly49q$_1^{neo}$* allele was electroporated with a CMV-Cre vector (a gift from D. Lohnes, University of Ottawa, Ottawa, Canada) and screened for neomycin deletion by PCR. *Ly49q$_1^{neo}$* and *Ly49q$_1^{lox}$* founder mice were generated by the IRCM MicroInjection Service. Founder mice that could transmit the targeted *Ly49q$_1$* allele to the germline were bred to 129S1 females to maintain a 129 background, which was confirmed for the *Ly49* locus by 4E5 versus 12A8 staining of NK cells, as previously described (38). The resulting heterozygous mice were bred, and homozygous WT and Ly49Q-null littermates were used in all experiments unless otherwise indicated. Southern blot analysis for the *Ly49q^{neo}* allele was performed using an intron 4 probe cloned into pCR2.1TOPO (Invitrogen), prepared by amplifying BAC 34o6 DNA with 5′-TATGACTTCTTGGAGAGAGT-3′ (sense primer) and 5′-TTCACGTGGGCCTAGAATTT-3′ (antisense primer). The *Ly49q$_1^{lox}$* allele was detected by PCR with 5′-CCTAAAAGTA-ATTGCTGTGACTATT-3′ (sense primer) and 5′-CTTTCTAAC-TAGCTAACAACAG-3′ (antisense primer). A substitute reverse primer, 5′-CCGAATATCATGGTGGAAAATGGC-3′, was used to amplify the *Ly49q$_1^{neo}$* allele. The following PCR cycling parameters used were: 94°C for 30 s, 55.5°C for 30 s, and 72°C for 30 s, for 35 cycles.

pDC isolation and in vitro activation. Mouse spleens were injected with collagenase (Roche), minced, and incubated for 20 min at 37°C. After incubation, splenocytes were crushed in cold PBS-BSA-EDTA and strained through a 70-μM filter. RBCs were removed by incubation with ACK lysis buffer for 5 min at 4°C. Isolated splenocytes were maintained throughout the procedure in cold PBS-BSA-EDTA. Anti–mPDCA-1–conjugated microbead (Miltenyi Biotec) labeling was performed according to the manufacturer's protocol. Isolated pDCs were seeded at 100,000 cells per well in 200 μl of pDC medium (RPMI 1640, 10% FBS, pen/strep, L-glutamine, 2-β-mercaptoethanol) and cultured for 16 h at 37°C in 5% CO_2 in a humidified atmosphere in the presence of CpG-ODN 10103 or 2336 (Coley Pharmaceuticals), imiquimod, MCMV, or influenza at the indicated concentrations/PFU/hemagglutinin units. Supernatants were collected and frozen.

In vivo pDC activation. Mice were injected through the tail vein with CpG-ODN plus 1,2-dioleoyloxy-3-trimethylammonium-propane

(DOTAP; Roche) preparation (170 µl CpG-ODN diluted in sterile PBS plus 30 µl DOTAP) or imiquimod (R-837; InvivoGen) in 200 µl PBS. Mice were bled through the cheek vein at the indicated time points after injection. Serum was analyzed by ELISA.

Virus infections. Influenza strain A HK X31 H3N2 was a gift from T. Watts (University of Toronto, Toronto, Canada). MCMV (Smith strain) preparation, injection, and plaque assay were performed as previously described (39).

ELISAs. Mouse IFN-α was determined by sandwich ELISA. In brief, 96-well microtiter plates were coated overnight at 4°C with 5 µg/ml of rat anti–mouse IFN-α antibody (RMMA-1; PBL Biomedical Laboratories) diluted in 0.1 M of sodium carbonate buffer. Wells were blocked for 1 h with PBS/10% FBS and incubated for 2 h with samples or a recombinant mouse IFN-α standard (Sigma-Aldrich). IFN-α was detected with 100 ng/ml of polyclonal rabbit anti–mouse IFN-α antibody (PBL Biomedical Laboratories) for 24 h at room temperature, washed, and incubated for 1 h with a donkey anti–rabbit IgG conjugated to horseradish peroxidase (GE Healthcare), followed by 20 min in 3,3′,5,5′-tetramethylbenzidine substrate (Sigma-Aldrich), and 1 M H_2SO_4 was added to stop the reaction. Between incubations, plates were washed three times with PBS/0.05% Tween-20. Optical density was read at 450 nm with a microtiter plate reader (MDS Analytical Technologies). IL-12p70, IL-6, and TNF-α production by pDCs was assayed using commercial ELISA kits (BD).

Immunofluorescence and FACS analysis. The following FACS mAbs were used: biotin-440c (anti–Siglec-H; Cell Sciences), allophycocyanin–mPDCA-1 (anti-BST2; Miltenyi Biotec), FITC-CD86, 2E6 (anti-Ly49Q; eBioscience), allophycocyanin-B220, PE-CD11c, and streptavidin-PE were purchased from BD. NS-34 (anti-Ly49Q) was prepared as previously described (10). PE-conjugated H-2K^b/OVA tetramer contains human β2 microglobulin and was purchased from Beckman Coulter. For all FACS analyses, cells were first washed in FACS buffer (PBS, 0.5% BSA, 0.02% NaN_3), and were then incubated for 20 min at 4°C with fluorochrome-conjugated antibodies. Two-step staining involved an additional incubation for 20 min with the appropriate secondary antibody at 4°C, followed by a wash in FACS buffer. Stained cells were analyzed with a flow cytometer (FACSCalibur; BD). Three-color immunofluorescent staining with biotin–rat anti–mPDCA-1 plus streptavidin-Alexa Fluor 594, hamster anti-CD3ε (BD) plus Alexa Fluor 647–goat anti–hamster IgG (Invitrogen), and FITC–anti-CD19 (BD) was performed on slide-mounted 10-µm spleen sections from untreated and CpG-ODN–injected mice. Slides were viewed on a confocal microscope (Axiovert 100M; Car Zeiss, Inc.).

Giemsa staining. Fresh or CpG-ODN–cultured pDCs were cytocentrifuged onto glass slides, fixed in methanol for 10 min, and air dried. Slides were stained with modified Giemsa stain solution (Sigma-Aldrich) diluted 1:10 in distilled H_2O for 10 min, rinsed with distilled H_2O, and mounted. Pictures were obtained with a microscope (Axiophot; Carl Zeiss, Inc.).

Statistical analysis. Unless otherwise indicated, all P values were calculated with the two-tailed Student's *t* test.

We thank Dr. P. Liu for assistance with BAC recombineering; Dr. Q. Zhu for ES cell selection and blastocyst injections; Drs. S.K. Anderson and A. Veillette for helpful discussion; Drs. J. Carlyle, W.-K. Suh, J. Di Noia, and J.-F. Coté for critical reading of the manuscript; and É. Massicotte and M. Dupuis for cell sorting.

This work was supported by an operating grant (MOP 62841) from the Canadian Institutes of Health Research (CIHR). L-H. Tai is supported by a CIHR Cancer Training Program scholarship. S. Belanger is supported by a Fonds de la recherche en santé Québec scholarship. A.P. Makrigiannis is supported by a New Investigator Award from the CIHR.

The authors have no conflicting financial interests.

Submitted: 4 April 2008
Accepted: 14 November 2008

REFERENCES

1. Liu, Y.J. 2005. IPC: professional type 1 interferon-producing cells and plasmacytoid dendritic cell precursors. *Annu. Rev. Immunol.* 23:275–306.
2. Facchetti, F., C. Wolf-Peeters, D.Y. Mason, K. Pulford, J.J. van den Oord, and V.J. Desmet. 1988. Plasmacytoid T cells. Immunohistochemical evidence for their monocyte/macrophage origin. *Am. J. Pathol.* 133:15–21.
3. Abb, J., H. Abb, and F. Deinhardt. 1984. Relationship between natural killer (NK) cells and interferon (IFN) alpha-producing cells in human peripheral blood. Studies with a monoclonal antibody with specificity for human natural killer cells. *Immunobiology.* 167:359–364.
4. Perussia, B., V. Fanning, and G. Trinchieri. 1985. A leukocyte subset bearing HLA-DR antigens is responsible for in vitro alpha interferon production in response to viruses. *Nat. Immun. Cell Growth Regul.* 4:120–137.
5. Kadowaki, N., S. Ho, S. Antonenko, R.W. Malefyt, R.A. Kastelein, F. Bazan, and Y.J. Liu. 2001. Subsets of human dendritic cell precursors express different Toll-like receptors and respond to different microbial antigens. *J. Exp. Med.* 194:863–869.
6. Asselin-Paturel, C., G. Brizard, J.J. Pin, F. Briere, and G. Trinchieri. 2003. Mouse strain differences in plasmacytoid dendritic cell frequency and function revealed by a novel monoclonal antibody. *J. Immunol.* 171: 6466–6477.
7. Nakano, H., M. Yanagita, and M.D. Gunn. 2001. CD11c$^+$B220$^+$Gr-1$^+$ cells in mouse lymph nodes and spleen display characteristics of plasmacytoid dendritic cells. *J. Exp. Med.* 194:1171–1178.
8. Asselin-Paturel, C., A. Boonstra, M. Dalod, I. Durand, N. Yessaad, C. Dezutter-Dambuyant, A. Vicari, A. O'Garra, C. Biron, F. Briere, and G. Trinchieri. 2001. Mouse type I IFN-producing cells are immature APCs with plasmacytoid morphology. *Nat. Immunol.* 2:1144–1150.
9. Blasius, A., W. Vermi, A. Krug, F. Facchetti, M. Cella, and M. Colonna. 2004. A cell-surface molecule selectively expressed on murine natural interferon-producing cells that blocks secretion of interferon-alpha. *Blood.* 103:4201–4206.
10. Toyama-Sorimachi, N., Y. Tsujimura, M. Maruya, A. Onoda, T. Kubota, S. Koyasu, K. Inaba, and H. Karasuyama. 2004. Ly49Q, a member of the Ly49 family that is selectively expressed on myeloid lineage cells and involved in regulation of cytoskeletal architecture. *Proc. Natl. Acad. Sci. USA.* 101:1016–1021.
11. Kamogawa-Schifter, Y., J. Ohkawa, S. Namiki, N. Arai, K. Arai, and Y. Liu. 2005. Ly49Q defines 2 pDC subsets in mice. *Blood.* 105:2787–2792.
12. Blasius, A.L., M. Cella, J. Maldonado, T. Takai, and M. Colonna. 2006. Siglec-H is an IPC-specific receptor that modulates type I IFN secretion through DAP12. *Blood.* 107:2474–2476.
13. Blasius, A.L., E. Giurisato, M. Cella, R.D. Schreiber, A.S. Shaw, and M. Colonna. 2006. Bone marrow stromal cell antigen 2 is a specific marker of type I IFN-producing cells in the naive mouse, but a promiscuous cell surface antigen following IFN stimulation. *J. Immunol.* 177:3260–3265.
14. Wilhelm, B.T., L. Gagnier, and D.L. Mager. 2002. Sequence analysis of the Ly49 cluster in C57BL/6 mice: a rapidly evolving multigene family in the immune system. *Genomics.* 80:646–661.
15. Makrigiannis, A.P., A.T. Pau, P.L. Schwartzberg, D.W. McVicar, T.W. Beck, and S.K. Anderson. 2002. A BAC contig map of the Ly49 gene cluster in 129 mice reveals extensive differences in gene content relative to C57BL/6 mice. *Genomics.* 79:437–444.
16. Proteau, M.-F., E. Rousselle, and A.P. Makrigiannis. 2004. Mapping of the BALB/c Ly49 cluster defines a minimal natural killer cell receptor gene repertoire. *Genomics.* 84:669–677.
17. Toyama-Sorimachi, N., Y. Omatsu, A. Onoda, Y. Tsujimura, T. Iyoda, A. Kikuchi-Maki, H. Sorimachi, T. Dohi, S. Taki, K. Inaba, and H. Karasuyama. 2005. Inhibitory NK receptor Ly49Q is expressed on subsets of dendritic cells in a cellular maturation- and cytokine stimulation-dependent manner. *J. Immunol.* 174:4621–4629.
18. Makrigiannis, A.P., D. Patel, M.L. Goulet, K. Dewar, and S.K. Anderson. 2005. Direct sequence comparison of two divergent class I MHC natural killer cell receptor haplotypes. *Genes Immun.* 6:71–83.
19. Omatsu, Y., T. Iyoda, Y. Kimura, A. Maki, M. Ishimori, N. Toyama-Sorimachi, and K. Inaba. 2005. Development of murine plasmacytoid dendritic cells defined by increased expression of an inhibitory NK receptor, Ly49Q. *J. Immunol.* 174:6657–6662.

20. Colonna, M., G. Trinchieri, and Y.J. Liu. 2004. Plasmacytoid dendritic cells in immunity. *Nat. Immunol.* 5:1219–1226.
21. Tai, L.H., M.L. Goulet, S. Belanger, A.D. Troke, A.G. St Laurent, A. Mesci, N. Toyama-Sorimachi, J.R. Carlyle, and A.P. Makrigiannis. 2007. Recognition of H-2K(b) by Ly49Q suggests a role for class Ia MHC regulation of plasmacytoid dendritic cell function. *Mol. Immunol.* 44:2638–2646.
22. Fuchs, A., M. Cella, T. Kondo, and M. Colonna. 2005. Paradoxic inhibition of human natural interferon-producing cells by the activating receptor NKp44. *Blood.* 106:2076–2082.
23. Asselin-Paturel, C., G. Brizard, K. Chemin, A. Boonstra, A. O'Garra, A. Vicari, and G. Trinchieri. 2005. Type I interferon dependence of plasmacytoid dendritic cell activation and migration. *J. Exp. Med.* 201:1157–1167.
24. Krug, A., A.R. French, W. Barchet, J.A. Fischer, A. Dzionek, J.T. Pingel, M.M. Orihuela, S. Akira, W.M. Yokoyama, and M. Colonna. 2004. TLR9-dependent recognition of MCMV by IPC and DC generates coordinated cytokine responses that activate antiviral NK cell function. *Immunity.* 21:107–119.
25. Tabeta, K., P. Georgel, E. Janssen, X. Du, K. Hoebe, K. Crozat, S. Mudd, L. Shamel, S. Sovath, J. Goode, et al. 2004. Toll-like receptors 9 and 3 as essential components of innate immune defense against mouse cytomegalovirus infection. *Proc. Natl. Acad. Sci. USA.* 101:3516–3521.
26. Lee, S.H., J. Gitas, A. Zafer, P. Lepage, T.J. Hudson, A. Belouchi, and S.M. Vidal. 2001. Haplotype mapping indicates two independent origins for the Cmv1s susceptibility allele to cytomegalovirus infection and refines its localization within the Ly49 cluster. *Immunogenetics.* 53:501–505.
27. Lee, S.H., S. Girard, D. Macina, M. Busa, A. Zafer, A. Belouchi, P. Gros, and S.M. Vidal. 2001. Susceptibility to mouse cytomegalovirus is associated with deletion of an activating natural killer cell receptor of the C-type lectin superfamily. *Nat. Genet.* 28:42–45.
28. Brown, M.G., A.O. Dokun, J.W. Heusel, H.R. Smith, D.L. Beckman, E.A. Blattenberger, C.E. Dubbelde, L.R. Stone, A.A. Scalzo, and W.M. Yokoyama. 2001. Vital involvement of a natural killer cell activation receptor in resistance to viral infection. *Science.* 292:934–937.
29. Nakamura, M.C., E.C. Niemi, M.J. Fisher, L.D. Shultz, W.E. Seaman, and J.C. Ryan. 1997. Mouse Ly-49A interrupts early signaling events in natural killer cell cytotoxicity and functionally associates with the SHP-1 tyrosine phosphatase. *J. Exp. Med.* 185:673–684.
30. Mason, L.H., J. Willette-Brown, A.T. Mason, D. McVicar, and J.R. Ortaldo. 2000. Interaction of Ly-49D+ NK cells with H-2Dd target cells leads to Dap-12 phosphorylation and IFN-gamma secretion. *J. Immunol.* 164:603–611.
31. Sjolin, H., S.H. Robbins, G. Bessou, A. Hidmark, E. Tomasello, M. Johansson, H. Hall, F. Charifi, G.B. Karlsson Hedestam, C.A. Biron, et al. 2006. DAP12 signaling regulates plasmacytoid dendritic cell homeostasis and down-modulates their function during viral infection. *J. Immunol.* 177:2908–2916.
32. Hamerman, J.A., N.K. Tchao, C.A. Lowell, and L.L. Lanier. 2005. Enhanced Toll-like receptor responses in the absence of signaling adaptor DAP12. *Nat. Immunol.* 6:579–586.
33. Hamerman, J.A., J.R. Jarjoura, M.B. Humphrey, M.C. Nakamura, W.E. Seaman, and L.L. Lanier. 2006. Cutting edge: inhibition of TLR and FcR responses in macrophages by triggering receptor expressed on myeloid cells (TREM)-2 and DAP12. *J. Immunol.* 177:2051–2055.
34. Kim, S., J. Poursine-Laurent, S.M. Truscott, L. Lybarger, Y.J. Song, L. Yang, A.R. French, J.B. Sunwoo, S. Lemieux, T.H. Hansen, and W.M. Yokoyama. 2005. Licensing of natural killer cells by host major histocompatibility complex class I molecules. *Nature.* 436:709–713.
35. Fernandez, N.C., E. Treiner, R.E. Vance, A.M. Jamieson, S. Lemieux, and D.H. Raulet. 2005. A subset of natural killer cells achieves self-tolerance without expressing inhibitory receptors specific for self-MHC molecules. *Blood.* 105:4416–4423.
36. Muller, U., U. Steinhoff, L.F. Reis, S. Hemmi, J. Pavlovic, R.M. Zinkernagel, and M. Aguet. 1994. Functional role of type I and type II interferons in antiviral defense. *Science.* 264:1918–1921.
37. Liu, P., N.A. Jenkins, and N.G. Copeland. 2003. A highly efficient recombineering-based method for generating conditional knockout mutations. *Genome Res.* 13:476–484.
38. Makrigiannis, A.P., A.T. Pau, A. Saleh, R. Winkler-Pickett, J.R. Ortaldo, and S.K. Anderson. 2001. Class I MHC-binding characteristics of the 129/J Ly49 repertoire. *J. Immunol.* 166:5034–5043.
39. Desrosiers, M.P., A. Kielczewska, J.C. Loredo-Osti, S.G. Adam, A.P. Makrigiannis, S. Lemieux, T. Pham, M.B. Lodoen, K. Morgan, L.L. Lanier, and S.M. Vidal. 2005. Epistasis between mouse Klra and major histocompatibility complex class I loci is associated with a new mechanism of natural killer cell-mediated innate resistance to cytomegalovirus infection. *Nat. Genet.* 37:593–599.